Astron. Astrophys. 314, 182–190 (1996)

ASTRONOMY AND ASTROPHYSICS

Whole Earth Telescope observations and seismological analysis of the cool ZZ Ceti star GD 154

B. Pfeiffer[1,3], G. Vauclair[1], N. Dolez[1], M. Chevreton[2], J.-R. Fremy[2], M. Barstow[3,11], J.A. Belmonte[4], S.O. Kepler[5], A. Kanaan[5], O. Giovannini[5], G. Fontaine[6,12], P. Bergeron[6,12], F. Wesemael[6,12], A.D. Grauer[7], R.E. Nather[8], D.E. Winget[8], J. Provencal[8,13], J.C. Clemens[8,14], P.A. Bradley[8,15], J. Dixson[8], S.J. Kleinman[8], T.K. Watson[8], C.F. Claver[8], T. Matzeh[9], E.M. Leibowitz[9], and P. Moskalik[10]

[1] Université Paul Sabatier, Observatoire Midi-Pyrénées, Laboratoire d'Astrophysique de Toulouse, 14 av. E. Belin, F-31400 Toulouse, France (gerard@obs-mip.fr)
[2] Observatoire de Paris, DAEC, F-92195 Meudon, France
[3] Department of Physics and Astronomy, University of Leicester, LE1 7RH, UK
[4] Instituto de Astrofisica, La Laguna, Tenerife, Spain
[5] Instituto de Fisica, Universidade Federal do Rio Grande do Sul, 91501-970 Porto Alegre, RS, Brazil
[6] Département de Physique, Universite de Montreal, CP6128, Succursale A, H3C 3J7, Montréal, Québec, Canada
[7] Department of Physics and Astronomy, University of Arkansas at Little Rock, Little Rock, AR 72204, USA
[8] Department of Astronomy, Univ. Texas, Austin, TX 78712, USA
[9] Department of Physics and Astronomy, University Tel Aviv, Ramat Aviv, Tel Aviv 69978, Israël
[10] Copernicus Astronomical Center, ul. Bartycka 18, PL-00716 Warsaw, Poland
[11] Guest Observer, Isaac Newton Telescope, Roque de Los Muchachos, La Palma, Spain
[12] Guest observer, Canada-France-Hawaï Telescope, Kamuela, Hawaii 96743, USA
[13] Present adress: University of Delaware, Physics and Astronomy Department, Sharp Lab., Newark, DE, 19716, USA
[14] Present adress: Department of Physics, Iowa State University, Ames, IA 50 011, USA
[15] Present adress: XTA, MS B-220, Los Alamos National Laboratory, Los Alamos, NM 87545, USA

Received 20 December 1995 / Accepted 29 March 1996

Abstract. This paper presents the results of high speed photometric observations of the cool variable DA white dwarf (DAV) GD 154 obtained with the Whole Earth Telescope. GD 154 is one of the coolest pulsating DA white dwarfs and its study is important for understanding the red edge of the ZZ Ceti instability strip. Its power spectrum is dominated by three independent modes ($P_1 = 1186.5s$, $P_2 = 1088.6s$ and $P_3 = 402.6s$), and their harmonics and linear combinations. None of the half-integer harmonics reported in previous observations were present during the WET campaign. We propose that the observed modes are trapped in the thin outer hydrogen layers. From the resulting identification of the pulsation modes, one derives an estimate of the rotation period (2.3 days) and of the mass of the outer hydrogen layer ($2 \times 10^{-10} M_*$).

Key words: white dwarfs – stars: oscillations – stars: interiors – stars: individual (GD 154)

1. Introduction

Since the discovery of the first variable white dwarf (HLTau76, Landolt 1968), the field of white dwarf seismology has known crucial improvements, both on the observational and theoretical points of view. Only a few of the known white dwarfs are luminosity variables - those with surface temperatures that yield maximum opacity for their atmospheric composition - but they are otherwise normal white dwarfs (Mc Graw, 1979; Winget, 1988). The result of the seismological investigation of their structure can be applied to white dwarfs in general, constraining the prior evolution of their progenitors.

The luminosity variations of white dwarfs result from non-radial g-mode pulsations driven by the $\kappa-\gamma$ mechanism located in the outer layers. The oscillations provide a view beneath the photosphere, and contain information about basic parameters such as the mass, chemical composition profile, rotation period and magnetic field strength.

Before we can use the tools of pulsation theory to probe the white dwarf's interior structure, we must disentangle the observed frequency structure from the observed light curve. It requires continuous high speed photometry with a network of telescopes located at various longitudes to minimize gaps in the time series data. The network is known as the Whole Earth Telescope (WET; Nather et al. 1990).

GD 154 (BG Canum Venaticorum) is a member of the class of pulsating white dwarfs known as the ZZ Ceti (or DAV) stars, which display intrinsic luminosity variations of a few percent

and periods ranging between 100 and 1200s. Only 24 ZZ Ceti stars are now known. The DAV instability strip is delineated by a narrow range in effective temperature along the white dwarf cooling sequence: $12,460K \geq T_{eff} \geq 11,160K$ according to the $ML2/\alpha = 0.6$ models of Bergeron et al., 1995 (ML2 describes the convection efficiency in the frame work of the mixing length theory and $\alpha = \ell/H_p$). The properties of the ZZ Ceti stars have been summarized by Winget and Fontaine (1982) and Winget (1988).

The variability of GD 154 was discovered by Robinson et al. (1978) who found that the light curve was dominated during nine consecutive nights by a single mode of moderate amplitude (hereafter f_1) with a period $P_1 = 1186s$. They suggested that such a long period belonged to a high overtone g-mode ($10 \leq k \leq 30$). The power spectrum exhibited harmonics of this dominant mode ($2f_1, 3f_1, 4f_1$ and $5f_1$). It also showed a series of peaks at frequencies close to half-integer subharmonics of the dominant mode ($1.52f_1, 2.53f_1$ and $3.53f_1$). In addition, during the last night of their ten days campaign, the light curve of GD 154 was dominated by the $1.52f_1$ subharmonic. This behaviour is reminiscent of some non linear dynamical systems. The occurence of half integer subharmonics of the dominant frequency is similar to what is observed in systems evolving toward a chaotic dynamical regime via a cascade of period doubling bifurcations. Such a behaviour has already been suspected in two cases from the analysis of the power spectrum of pulsating white dwarfs : for the DBV PG1351+489 (Winget et al. 1987; Goupil et al. 1988) and the DAV G191-16 (Vauclair et al. 1989). The drastic change of the dominant frequency from f_1 to $1.52f_1$ observed by Robinson et al. (1978) also points to the potential efficiency in GD 154 of a mechanism responsible for exchanging energy between these two modes, possibly through non-linear effects. Those peculiarities were a strong motivation to devote a Whole Earth Telescope campaign to GD 154.

Furthermore, GD 154 presents some other interesting peculiarities as a member of the DAV class. It is one of the coolest ZZ Ceti stars. Based on fits to the Balmer line profiles, Daou et al. (1990) determined an effective temperature of 11 320 K. However the UV flux (IUE) gives a temperature some 400 K hotter (Kepler and Nelan 1993). More recently, Bergeron et al. (1995) demonstrated how an internally consistent determination of both the effective temperature and the surface gravity requires the simultaneous fitting of optical and UV spectra. They showed how a unique version of the mixing length theory successfully achieved this requirement with ML2/α=0.6. According to their analysis, GD 154, with an effective temperature of 11 180 K, belongs to a group of three ZZ Ceti stars, which defines the red edge of the instability strip (with R808 and G38-29 at T_{eff} = 11 160 K and 11 180 K respectively). Their derived mass of 0.70 $M_\odot$ for GD 154, is significantly higher than the average mass of DA white dwarfs. It is also the most massive of the three ZZ Ceti defining the red edge.

The period of the dominant mode of GD 154 (1186 s) is the longest period up to now observed in a DAV. It is significantly longer than the periods of the dominant modes in G38-29 (1024 s) and R808 (833 s). Note that the location of the red edge as defined by these three stars does not depend on the total mass of the stars (Bergeron et al. 1995). If it is assumed that the observed modes are trapped modes in the hydrogen outer layers, the longer period in GD 154 compared to the other stars of the same effective temperature may have three different origins (Brassard et al. 1992b):

1- the outer hydrogen layer of GD 154 could be thinner: modes of higher k index are trapped,

2- the convection in the outermost layers of GD 154 could be more efficient (equivalent to a lower effective temperature)

3- GD 154 could be a low mass DA.

The third hypothesis cannot be the correct one since Bergeron et al., 1995 derive a mass of $0.70M_\odot$ for GD 154 against $0.55M_\odot$ for G38-29 and 0.63 $M_\odot$ for R808; the fact that GD 154 is the most massive of the three stars reinforces the first two propositions. As the best fit for the optical and UV spectra was obtained for a unique version of the MLT (ML2/α=0.6) there is no special reason to believe that GD 154 should behave differently than other ZZ Ceti stars. Therefore, the most likely explanation of the long period is that GD 154 has a thinner hydrogen envelope.

The physical origin of the instability strip red edge is still unknown. Three assumptions have been made to explain the abrupt red edge. The first one is that convective mixing of the outer hydrogen with the deeper helium envelope, when the convection zone reaches the H/He transition layer, should stop the pulsation as the driving mechanism (the κ-mechanism due to partial ionization of hydrogen) would not be efficient anymore. However, this would require an extremely thin and well tuned hydrogen outer layer mass ($M_H \sim 10^{-14}$ to 10^{-11} $M_\odot$ according to Fontaine and Wesemael 1991) to account for the same boundary in the above three DAVs defining the red edge. Furthermore, estimates of the hydrogen layer mass in a few hotter ZZ Ceti points to larger hydrogen mass than the one required to produce convective mixing at $\sim$ 11 200 K. The inferred hydrogen layer masses are $M_H = 10^{-4.4}$ M_* in G226-29, if the observed modes are $\ell = 1$ (Fontaine et al. 1992), $\geqq 10^{-3.7}$ M_* or $\geqq 10^{-6.4}$ M_* in GD165, depending on whether the observed modes are $\ell = 1$ or $\ell = 2$ respectively (Bergeron et al. 1993), and $\sim 10^{-8}$ M_* in PG2303+243 (Vauclair et al. 1992). The second assumption to explain the red edge invokes the increasing interaction between the pulsations and the convection which could ultimately damp the instability. Recent stability analyses including more realistic description of the convection than the standard mixing length theory and exploring various efficiency of the convection/pulsation coupling do conclude that such damping is possible for the lower frequency g-modes (Gautschy et al. 1996). However, this problem still requires considerable efforts on the theoretical side. A third assumption is that below a critical frequency, the leakage of the gravity waves upwards though the stellar atmosphere would damp the instability (Hansen et al. 1985). But the damping would be efficient for periods much longer than observed in the three DAVs defining the red edge,

Table 1. Journal of observations of the WET campaign

Observatory	Date (May 91)	started at (UT)	length (s)	Observatory	Date (May 91)	sarted at (UT)	length (s)
Mc Donald 82-in	13	06:09:30	12100	Mauna Kea 24-in	18	05:59:20	29005
Mc Donald 36-in	14	03:41:00	10980	OHP 1.93m	18	20:51:50	19020
Mc Donald 82-in	15	03:19:00	9880	Itajuba 1.60m	19	01:23:10	14630
Mauna Kea 24-in	15	06:10:20	2290	Mc Donald 36-in	19	02:59:00	23300
Mc Donald 82-in	15	07:30:10	7640	Mauna Kea 24-in	19	06:53:20	26070
Mauna Kea 24-in	15	08:11:50	17720	OHP 1.93m	19	21:05:30	16440
La Palma INT	16	00:27:30	13015	Mc Donald 36-in	20	03:04:20	22510
Mc Donald 36-in	16	02:55:00	23305	Mauna Kea 24-in	20	05:50:30	24150
Mauna Kea 24-in	16	07:31:50	23400	Mauna Kea CFHT	20	06:33:23	9990
Wise 40-in	16	18:35:11	1785	OHP 1.93m	20	21:09:00	18005
Wise 40-in	16	19:48:01	3635	Mauna Kea 24-in	21	09:51:00	13370
OHP 1.93m	16	21:48:37	16070	Wise 40-in	21	18:34:10	2025
Mc Donald 36-in	17	03:00:00	10775	OHP 1.93m	21	21:01:00	18968
Mauna Kea 24-in	17	06:10:20	26415	Mauna Kea CFHT	22	05:49:40	21600
Mc Donald 36-in	17	06:15:00	2735	OHP 1.93m	22	21:26:40	17640
Mc Donald 36-in	17	07:41:15	7260	Mc Donald 82-in	23	05:52:00	7720
Wise 40-in	17	18:44:01	2005	Mauna Kea CFHT	23	06:04:37	14400
Wise 40-in	17	19:30:31	5830	Mc Donald 82-in	24	03:41:10	10275
OHP 1.93m	17	20:59:30	18900	Mauna Kea CFHT	24	05:51:43	20920
Wise 40-in	17	21:50:21	2220	Mc Donald 36-in	25	03:15:00	21215
Mc Donald 36-in	18	02:57:00	15745				

namely $P_g \gtrsim 4200$ s for $\ell = 1$ modes and $P_g \gtrsim 2450$ s for $\ell = 2$ modes.

Consequently, GD 154 was considered to be an important target for a WET campaign. This campaign was organized in 1991 and the observations are described in Sect. 2. The power spectrum and the inferred rotational splitting are discussed in Sect. 3 and Sect. 4 respectively. An interpretation is given in Sect. 5. A short post WET observation of GD 154 is described in Sect. 6. The main conclusions of the paper are summarized in Sect. 7.

2. Observations

GD 154 (α_{2000} = 13 09 58, δ_{2000} = +35 09.5) was one of the two first priority targets of the May 1991 WET observing run. 162.5hrs of data were collected over 12 days from 6 observatories distributed in longitude (see Table 1 for the Journal of the observations). The resulting resolution of the Fourier Transform is 1μHz.

The method of data acquisition and reduction has been described by Nather et al.(1990). In most of the sites, data were obtained with 2-channel photometers: the observations of the target and the comparison star were interrupted at irregular intervals to sample the sky brightness as conditions warranted. The sky background contribution is then interpolated and subtracted. In the two sites where 3-channel photometers were used (OHP, CFHT), the third channel was continuously observing the sky background. For these data, the sky is subtracted on a point by point basis. The effect of extinction and other low frequency transparency variations were accounted for by fitting a third order polynomial to each sky-subtracted data set and then by dividing by this fit. The light curve is then obtained in terms of fractional amplitude: this method allows the use of the star as its own magnitude calibration for each telescope. The data acquired for the nearby comparison star in channel 2 were used to measure sky transparency. All light curves were sampled with a 10s integration time.

The data have been placed on a common BJD time scale. Barycentric correction was applied to each data point in order to correct the time delay introduced by the heliocentric motion of the Earth during the light curve acquisition. The final product of this basic reduction procedure is shown in Fig. 1.

All data contaminated by clouds were discarded. As there was no telescopes in Asia and because this WET campaign had two primary targets, the duty cycle for the whole campaign was only 48.8%.

3. The power spectrum

Fig. 2a, shows the Discrete Fourier Transform of the entire WET campaign. In Fig. 2b, one can see the corresponding spectral window which is the power spectrum of a sine function sampled in the same way as the data. To make easier the comparison with the observed power spectrum, the amplitude and the frequency of the sine function were chosen to equal those of the main peak in Fig. 2a.

The power spectrum does not exhibit any significant signal for frequencies higher than 5 mHz. The noise level of the ob-

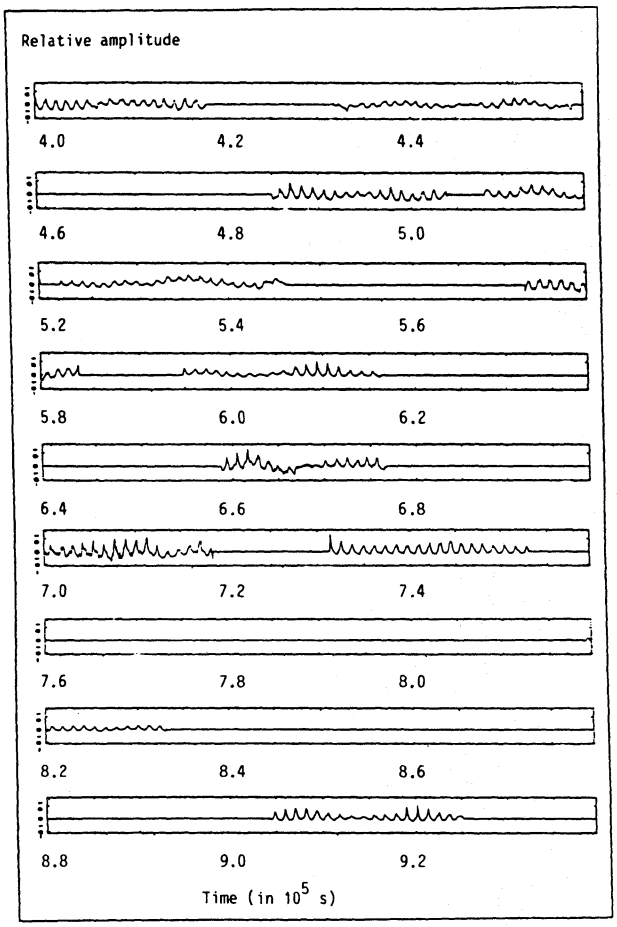

Fig. 1. Light curve of GD 154 during the central part of the WET campaign. The relative amplitude is plotted versus the time in sec.

Table 2. Frequencies, periods and amplitudes of WET power spectrum peaks

Frequency (μHz)	Period (s)	Amplitude (%)	Interpretation
840.0	1190.5	0.63	f_1^-
842.8	1186.5	1.67	f_1
845.0	1183.5	0.46	f_1^+
(916	1092	0.30	f_2^-)
918.6	1088.6	0.50	f_2
922.5	1084.0	0.56	f_2^+
1683.2	594.1	0.39	($2.f_1^-$)
1686.2	593.1	0.21	$2f_1$
1759.9	568.2	0.11	f_1+f_2
1765.2	566.5	0.13	$f_1+f_2^+$
1823.4	548.4	0.11	-
1837.7	544.2	0.18	$2f_2$
2484.1	402.56	0.27	f_3
2518.6	397.05	0.08	$3.f_1^-$
2526.2	395.86	0.09	($3f_1$)
2597.5	384.98	0.08	$2f_1^-+f_2$
2680.2	373.10	0.08	f_1+2f_2
3323.3	300.90	0.07	f_3+f_1m
3327.0	300.57	0.16	f_3+f_1
3406.4	293.57	0.06	-
3448.4	289.99	0.05	$3f_1+f_2$
4169.8	239.82	0.06	f_3+2f_1

served power spectrum begins to rise, roughly exponentially, below 0.5 mHz, thus diluting any signal that might be present.

In order to examine the WET data more deeply, and to distinguish real peaks from false ones introduced by the sidelobes of the spectral window, the FT has been deconvolved using two different methods. One runs in the time domain (ISWF, Ponman, 1981) and the second in the frequency domain (based on the CLEAN method, Högbom, 1974). In each case, all the peaks belonging to a given "forest" of peaks are deconvolved simultaneously in order to avoid propagating errors in the computation of the amplitudes and phases of the injected sine waves. Both methods gave comparable results. Table 2 lists the frequencies, periods and amplitudes of the peaks extracted from the WET power spectrum by these procedures.

The WET power spectrum contains only three independent modes: $f_1 = 842.8\mu$Hz , $f_2 = 918.6\mu$Hz and $f_3 = 2484.1\mu$Hz. All the other peaks except two can be interpreted as harmonics and linear combinations of these three main peaks. f_1 and f_2 appear to be triplets which will be discussed below (Sect. 4). The frequency f_3 is close to the second harmonic of f_1 ($3f_1 = f_3 + 44.3\mu$Hz) so that linear combinations of f_1 and f_3 can mimic high order harmonics of f_1 in lower resolution data.

A comparison of the WET spectrum with the observations performed 14 years earlier by Robinson et al. (1978), reveals drastic changes. The power spectrum was then dominated by a single mode and its integer and 'half-integer' harmonics. It could also be interpreted as two modes (f_1 and $1.52f_1$) and their harmonics and linear combinations. In the WET data, two new modes appear, one close to f_1 (f_2) and the other one close to $3f_1$ (f_3). The striking result of the WET campaign is that there is no evidence for peaks around $1.52f_1$, not even in the power spectra of individual nights. Comparing the individual power spectra of every observing night, it appears that the amplitude variations of f_1 and f_2 seem to be anticorrelated. This suggests that in May 1991, the mode f_1 was exchanging energy with the other dominant mode f_2. In order to have a qualitative idea of the life time of coherent structures in the signal, a matching pursuit time frequency analysis (Mallat and Zhang, 1993) was performed on the individual observing runs, paying particular attention to the time-frequency diagrams of high signal-to-noise ratio CFHT observations. This analysis reveals that the mode f_3 is not a stable mode: on the May 22 CFHT run, it lasts the whole night but on May 24 , for example, the structure with a frequency f_3 appears only in the middle of the night, with a one hour lifetime. The power spectrum of the 4 CFHT observations alone reveals additional harmonics of f_1 and linear combinations

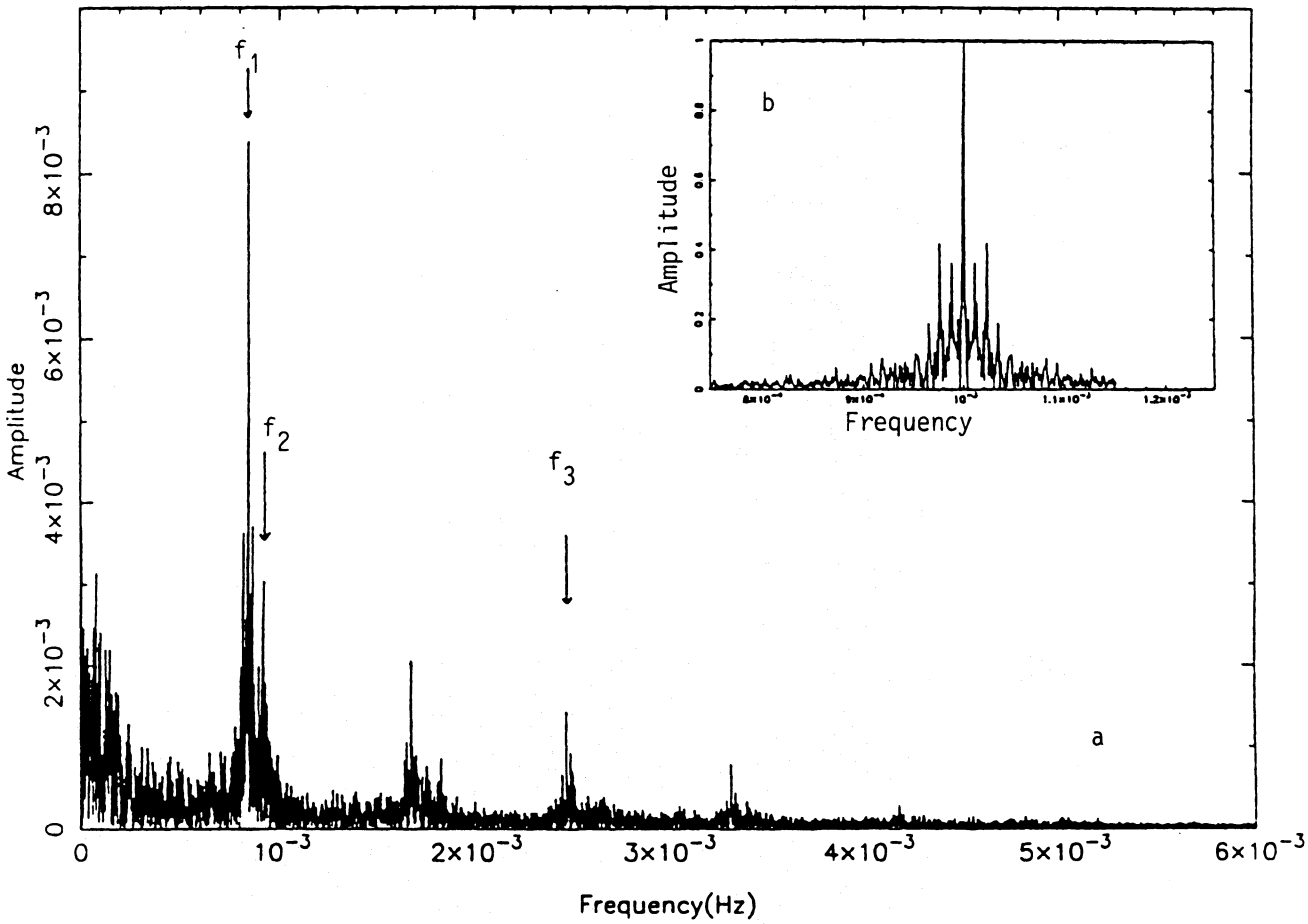

Fig. 2. a Fourier transform of the GD 154 WET data. The amplitude is plotted versus the frequency. The three independent frequencies are marked; **b** the spectral window corresponding to the WET campaign is shown on a enlarged scale. It is the Fourier transform of a noise free single sinusoid at frequency f_1 sampled at the same times as the data.

of frequencies undetected in the spectrum of the whole WET campaign at $2f_2 - f_1, 3f_2 - f_1, 4f_1, 2f_1 + 2f_2$ and $5f_1$. On individual good S/N observing runs even the components $2f_2^+ - f_1, f_3 - f_1$, $3f_2 - f_1$ are detected. All these features are the signature of the *non linear behaviour* of this object.

4. The rotational splitting

As one can see in Table 2, the WET observations reveal that the large amplitude region around f_1 (842.8 μHz) is actually a triplet, whose components are hereafter referred to as f_1^-, f_1 and f_1^+. This triplet is almost symmetric in amplitude and the frequency separations are $f_1 - f_1^- = 2.8\mu$Hz and $f_1^+ - f_1 = 2.2\mu$Hz. It is most naturally interpreted as a $\ell = 1$ g-mode split by rotation. For such a large period, one can resonably assume that the asymptotic regime (large k) is reached. For $\delta f_1 = 2.5\mu$Hz (average of the above frequency separations), a straightforward derivation of the rotation period of the star gives:

$$P_{rot} = \frac{1}{2.\delta f_1} = 2.3d \pm 0.3d$$

The mode f_1^- can be interpreted as the m= -1 component of the triplet, f_1 as the m=0 component and f_1^+ as the m=+1 component. The frequency asymmetry is only marginally significant; and will not be discussed any further.

The WET data reveal that the peak f_2 is composed of two components: f_2 (918.6 μHz) and f_2^+ (922.5 μHz) separated by 3.9 μHz. After subtraction of these 2 components, the power spectrum exhibits a third component at about 916μHz. However, the deconvolution gives a low level of confidence to the measurements of the frequency and amplitude of this third peak, as the window function has high sidelobes and because one has to deconvolve two peaks of higher amplitude (f_2 and f_2^+) before being able to detect it. This mode can be either the m=-1 component of the multiplet associated to f_2 or an independent mode. As the frequency of this mode is not accurately determined, it will not be used in the further interpretation.

5. Interpretation

The small number of observed eigenmodes does not give enough constraints to determine the basic physical parameters of this

object by comparing its eigenperiod distribution with pulsating white dwarf models. In order to interpret the observed power spectrum, it is necessary to impose other constraints. Among the rich spectrum of eigenperiods of GD 154, only three modes were accuratly detected in 1991, and two in 1977 (f_1 and $f_{rob} = 1.52 f_1$). An efficient mode selection mechanism is therefore at work. The most likely hypothesis, and the most developed in the literature, is that the observed modes are *trapped* in the outer hydrogen layer of the star (Winget et al., 1981; Dolez and Vauclair, 1981; Winget and Fontaine, 1982). These modes are characterized by a lower kinetic energy than the other eigenmodes. Fig. 20 of Brassard et al. (1992b) shows the kinetic energy of modes vs eigenperiod for different hydrogen layer masses. From this figure, one can see that the number of modes selected by mode trapping is very small and the trapping is *very* efficient for low hydrogen layer masses. These features match well the main characteristics of GD 154 power spectrum. If, on the other hand, it is assumed that GD 154 has a thick outer hydrogen layer, then the trapping would be much less efficient (specially for high k modes). The density of trapped modes would be much higher (up to 19 (12) $\ell = 1$ trapped modes with periods ranging from 100s to 1200s for a hydrogen mass layer of $10^{-4} M_*$ ($10^{-5} M_*$)) according to the models of Bradley (1996). If the hydrogen layer mass of GD 154 is 10^{-4} or 10^{-5} then it would have a structure similar to that of the hot DAVs with thick H layers. This still begs the question of a suitable mode selection mechanism, whether it be convection-pulsation interactions or a more complicated mode trapping resonance that involves the He/C or C/O transition regions. Bradley's numerical models are able to produce solutions that match the observed periods in both cases, but as a thin hydrogen layer is more likely from the point of view of kinetic energy arguments, this assumption is preferred to interpret GD 154 power spectrum.

Nevertheless, one must keep in mind that if one could establish that other stellar phenomena (such as convection) do provide another efficient selection mechanism, the interpretation should be re-examined. Gautschy et al. (1996) have recently explored the role of the convection on the stability of g-modes in ZZ Ceti white dwarfs. Their stellar models use a description of convection zone deduced from realistic 2D hydrodynamical simulations. The perturbation of the convective flux is taken into account according to various assumptions. Because the convection zones deduced from their 2D hydrodynamical simulations are much shallower than the ones derived from MLT, the "frozen-in" assumption for the convective flux is not able to produce the instability in the appropriate effective temperature range observed for the ZZ Ceti. It is only when the assumption of instantaneous adaptation of convection to the pulsation is made, with the additional constraint of the horizontal shear cancellation within the convection zone, that unstable g-modes are found. Even with this extreme assumption, the derived ZZ Ceti instability blue edge is still significantly cooler than the observed one. In spite of this difficulty, the fact that the convection damps many of the g-modes, which would otherwise be unstable with the use of the MLT to describe the convection, is an indication that both trapping and convection/pulsation coupling could be responsible for the small number of modes observed in ZZ Ceti stars. Considering the rather preliminary state of the art of this long debated question of the convection/pulsation coupling, we conservatively consider that mode trapping is the dominant mode selection mechanism.

Assuming that the mode f_1 (period P_1) is $\ell = 1$, one can try to determine the value of the ℓ index of the mode f_2 (period P_2). First, let us assume that f_2 is a mode $\ell = 1$. Then, the difference of the reduced periods ($\tilde{P} = \sqrt{(l(l+1))} P_l$) between P_1 and P_2 is:

$$\Delta\tilde{P} = \sqrt{2}.(P_1 - P_2) = 138.5s$$

Following Brassard et al.'s thin hydrogen layer models (1992a), such a $\Delta\tilde{P}$ is too small for these two modes to belong to two successive trapping valleys; it is also too large for P_2 to be the $\ell = 1$ mode adjacent to P_1, partially trapped in the trapping valley as P_1 . As f_2 cannot be a trapped $\ell = 1$ mode, it is assumed that P_2 is a mode $\ell = 2$. f_2 and f_2^+ are likely to belong to the same multiplet (same ℓ, consecutive m) with a separation of 3.9 μHz between the visible components due to rotational splitting. The other components, except the f_2^- discussed above (Sect. 4), are not detected. In such a case, the ratio of the frequency separations in the multiplets f_1 and f_2 has to be close to the theoretical ratio expected for a multiplet $\ell = 1$ and a multiplet $\ell = 2$ in the asymptotic regime ($\delta f_{l=1}/\delta f_{l=2} = 0.6$). Here, one gets:

$$\frac{\delta f 1}{\delta f_2} = \frac{2.5}{3.9} = 0.64$$

which is consistent with the hypothesis that f_2 could be a mode $\ell = 2$. However, this is not a very strong argument as the f_2^- frequency is not determined with sufficient accuracy to derive a better average value of the f_2 multiplet frequency separation. The small number of components detected in this multiplet does not allow to assign uniquely their m index.

A frequency asymmetry within multiplets is frequently observed in DAV power spectra. In the case of noisy data and high sidelobe spectral window such an asymmetry should not be over interpreted, as it can be due to deconvolution errors. It should be emphasized that finding a family of frequencies, amplitudes and phases that enable us to compute a synthetic power spectrum very "similar" to the observed one does not *prove* that the solution obtained is the best one. This is important in the case of noisy data where one can find many solutions leading to a synthetic power spectrum "similar" to the observed one.

An amplitude asymmetry within multiplets is also often observed in DAVs power spectra. In GD 154, the triplets are too strongly asymmetric to allow an estimate of the angle between the axis of pulsations and the line of sight, which is possible if one assumes that all components of a given multiplet have the same intrinsic amplitudes (as proposed by Pesnell, 1985).

Having identified the modes f_1 and f_2 as $\ell = 1$ and $\ell = 2$ modes, the ℓ index of the modes f_3 (period P_3) and $f_{rob} = 1.52 f_1$ (period $P_{rob} = 781s$) has to be determined.

Fig. 15 of Brassard et al. (1992a) gives the period spectrum for trapped modes in terms of the hydrogen layer mass for $\ell = 1$,

$\ell = 2$ and $\ell = 3$ g-modes. Their plot was performed for their reference model (12,500K, 0.6 $M_\odot$,ML1) but using their semi-analytic formula (28), one can draw an equivalent diagram for any T_{eff} and M_* not too far from their reference values, as well as for a higher convection efficency. Doing so for $T_{eff} = 11,180K$ and $M_* = 0.70 M_\odot$ and a convection efficency ML2, and after discarding the unlikely $\ell = 3$ solutions, leads to the conclusion that the solution the more likely to match our observations gives for P_3, P_{rob}, and P_1 three $\ell = 1$ modes of successive trapping indexes i=1, i=2 and i=3 respectively. On such a diagram, P_2 is matched with a trapping index i=5.

According to Clemens (1993), considerations based on the comparison of the power spectra of the 24 known ZZCeti stars also suggest that the mode P_3 is an independent $\ell = 1$ mode. Hence "half-integer" subharmonics observed by Robinson et al.(1978) could simply be the linear combinations of the frequencies of two *l*=1 *trapped modes*: the main mode (f_1), corresponding to the third trapping valley (i=3), and the mode $1.52f_1$, corresponding to the second trapping valley (i=2).

With the suggested identification for ℓ and i indexes of the independent modes, one can use the relation (28) of Brassard et al. 1992a:

$$\left(\frac{M_*}{M_\odot}\right)^{1.079}\left(\frac{M_H}{M_*}\right)^{0.102}\left(\frac{T_{eff}}{11,500K}\right)^{0.262} = \frac{1}{14.34}$$

together with the determination of $T_{eff} = 11,180K$ and $M_* = 0.70\ M_\odot$ derived by Bergeron et al. (1995), and for a ML2 convection efficiency, to obtain a hydrogen layer mass (M_H/M_*) between 1×10^{-10} and 3×10^{-10}. This value of the hydrogen outer layer would make GD 154 the ZZ Ceti with the thinnest hydrogen envelope so far. This hydrogen layer mass is however still too large to support the proposition that the red edge of the instability strip could be due to convective mixing of the outer hydrogen with the helium underneath.

6. Post WET observations

In order to examine the behaviour of GD 154 one month after the WET observations, a bi-site observing campaign was organized in June 1991. Table 3 gives the journal of these observations. All the observations were performed with 3-channel photometers: the Chevreton photometer in Izania and the Lepus photometer on Mt Bigelow. The June data were analysed independently in order to check the stability of GD 154's power spectrum on a time scale of one month. Due to poor meteorological conditions, the temporal coverage of this campaign was only 11.8%; the frequency resolution is 1.8μHz. The power spectrum of this campaign is given in figure 3-a and the spectral window in figure 3-b. The comparison of the June spectrum with the WET power spectrum shows that:

1- the main features of the spectrum obtained during the WET campaign ($f_1, f_2, 2f_1, f_1+f_2, 2f_2, f_3, f_3+f_1, f_3+2f_1$) are still present

2- there is still no evidence for a mode around $1.52f_1$

Table 3. Post-WET campaign, journal of observations

Observatory	Date (June 91)	started at (UT)	length (s)
Mt Bigelow(1.5m)	06	06:49:00	6900
Mt Bigelow(1.5m)	07	04:04:00	15960
Izania(1.5m)	07	21:31:05	14850
Mt Bigelow (1.5m)	08	03:38:00	17080
Izania(1.5m)	12	21:27:05	12310

Table 4. Identification of the independent eigenmodes in GD 154

mode	l	m	i
f_1^-	1	−1	3
f_1	1	0	3
f_1^+	1	+1	3
f_2	2	–	5
f_2^+	2	–	5
$1.52f_1$	1	–	2
f_3	1	–	1

If the eigenmodes excited in GD 154 are very different on a timescale of fourteen years, there is no evidence of drastic excitation or damping of modes on a timescale of one month. Accordingly, the times scales involved in the power spectrum variation of GD 154 need to be documented by more photometric observations. No one-day change of the kind observed in the 1977 observations by Robinson et al. (1978) was observed either during the 10 days WET campaign or during the post-WET observations one month later.

The coverage of the whole set of data (May and June) is so incomplete that it is not possible to put the two campaigns head to tail to improve the frequency resolution of the WET campaign as none of the known deconvolution methods can give reliable results in such a case.

7. Conclusions

The Whole Earth Telescope has been used to perform a detailed asteroseismological investigation of a variable DA white dwarf. During the WET observations, the behaviour of GD 154 was dominated by three independent eigenmodes. The data are interpreted under the reasonable assumption that all the observed modes are trapped in the outer hydrogen layer. An identification of their asteroseismological indexes ℓ and i, as well as those of the eigenmode observed 14 years earlier by Robinson et al.(1978), are summarized in Table 4. With the help of two more constraints derived from spectroscopic measurements by Bergeron et al. (1995) (T_{eff} and M_*), an estimate of the hydrogen layer mass $M_H = 2(\pm 1) \times 10^{-10} M_*$ is proposed. It should be reminded that this interpretation may not be unique: it relies on the assumption that the dominant selection mechanism at work in GD 154 is mode trapping in the hydrogen outer layers.

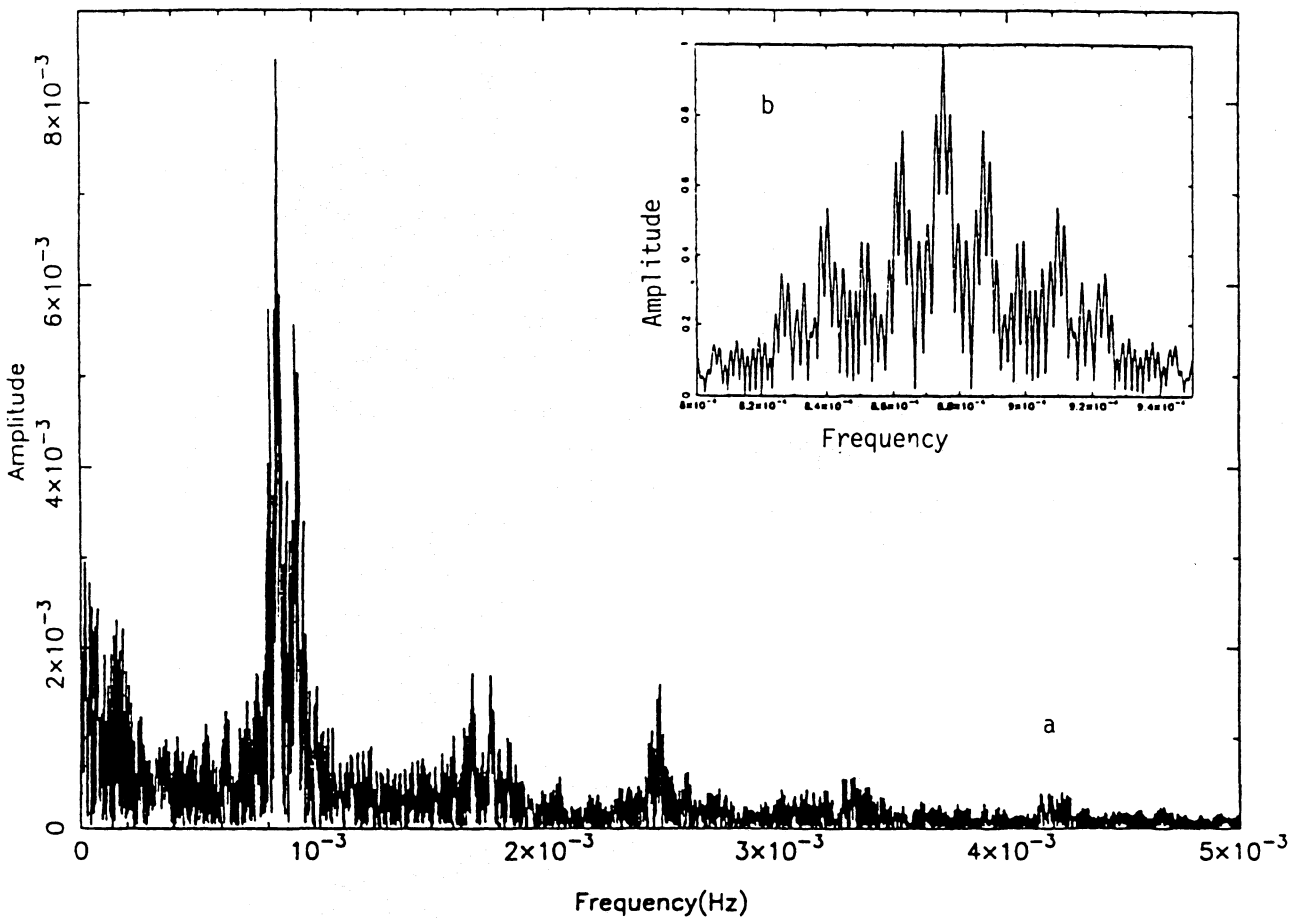

Fig. 3a and b. Same as Fig. 2 but for the post-WET observations; **a** the Fourier transform shows the same structure as in Fig. 2a; **b** the spectral window does reflect the poor coverage of the observations.

The behaviour of this object (using monosite campaigns) needs to be followed carefully in order to detect new drastic changes in its pulsation modes. New tools have also to be developed to understand its non linear behaviour: accurate time-frequency analysis enabling to describe quantitatively the amplitude variations of the individual modes and theoretical tools to describe the nonlinear terms observed in the power spectrum of this object.

Acknowledgements. We would like to thank Bertrand Serre and Sylvie Roques for running the Matching Pursuit algorithm on our data. G. Fontaine, P. Brassard and F. Wesemael acknowledge support from the NSERC Canada and the Fund FCAR (Québec).

References

Bergeron et al. 1993, AJ 196, 1987
Bergeron, P., Wesemael, F., Lamontagne, R., Fontaine, G., Saffer, R.A. and Allard, N.F., 1995, ApJ 449, 258
Bradley, 1996, submitted
Brassard, P., Fontaine, G., Wesemael, F., Hansen, C.J., 1992 a, ApJS 80, 369
Brassard, P., Fontaine, G., Wesemael, F., Tassoul, M., 1992b, ApJS 81, 747
Clemens, J.C., 1993, Baltic Astronomy 2, 407
Daou, D., Wesemael, F., Bergeron, P., Fontaine, G., Holberg, J.B., 1990, ApJ 364, 242
Dolez, N., and Vauclair, G., 1981, A&A 102, 375
Fontaine, G., Brassard, P., Bergeron, P., Wesemael, F. 1992, ApJ 399, L91
Fontaine, G., Wesemael, F. 1991, in IAU Symp. 145, Evolution of Stars: The Stellar Abundance convection, ed. G. Michaud & A. Tutukov (Dordrecht: Reidel), 421
Gautschy, A., Ludwig, H.-G., Freytag, B. 1996, A&A in press
Goupil, M.-J., Auvergne, M., Baglin, A. 1988, A&A 196, L13
Hansen, C.J., Winget, D.E., Kawaler, S.D. 1985, ApJ 297, 544
Högbom,J.A., 1974, A&AS 15, 417
Kawaler, S.D., and Weiss,P., 1991, Progress of Seismology of the Sun and Stars, Proc. 9th International Seminar, ed. Osaki and Shibahashi, Berlin, Springer- Verlag, p. 431
Kepler, S.O. and Nelan, E.P., 1993, AJ 105, 608
Landolt, A.U. 1968, ApJ 153, 151
Mallat, S. and Zhang, Z., 1993, in Progress in Wavelet Analysis and Applications, ed. Meyer and Roques, Frontiéres, Gif-sur-Yvette, 155
McGraw, J.T., 1979, ApJ 229, 203
Nather, R.E., Winget, D.E., Clemens, J.C., Hansen,C.J., Hine, B.P. 1990, ApJ 361, 309
Pesnell, W.D., 1985, ApJ 292, 238

Ponman, T., 1981, MNRAS 196, 583
Robinson, E.L., Stover, R.J., Nather, R.E., and Mc Graw, J.T., 1978, Ap J, 220, 614
Vauclair, G., Goupil, M.-J., Baglin, A., Auvergne, M., Chevreton, M. 1989, A&A 215, L17
Vauclair, G., Belmonte, J.A., Pfeiffer, B., Grauer, H.D., Jimenez, A., Chevreton, M., Dolez, N., Vidal, O., Herpe, G. 1992, A&A 264, 547
Winget, D.E., Van Horn, H.M., Hansen, C. J., 1981, ApJ 245, L33
Winget, D.E., Nather, R.E., Hill, A.J. 1987, ApJ 316, 305
Winget, D.E., and Fontaine, G., 1982, in Pulsations in Classical and Cataclysmic Variable Stars, Ed. J.P. Cox and C.J. Hansen, Boulder: Univ. Colorado, 46
Winget, D.E., 1988 , in Christensen-Dalsgaard J., Frandsen, S., eds Proc IAU Symp 123, Advances in Helio- and Asteroseismology , Reidel, Dordrecht, 305

This article was processed by the author using Springer-Verlag TEX A&A macro package version 4.